Sensitivity of regional hydrology to climate changes, with application to the Illinois River basin

Jeffrey D. Niemann

Department of Civil Engineering, Colorado State University, Fort Collins, Colorado, USA

Elfatih A. B. Eltahir

Department of Civil and Environmental Engineering, Massachusetts Institute of Technology, Cambridge, Massachusetts, USA

Received 13 December 2004; revised 14 April 2005; accepted 26 April 2005; published 14 July 2005.

[1] This paper investigates the sensitivity of regional hydrology to climate change using a physically based model. The model partitions precipitation into surface runoff, groundwater runoff, and evapotranspiration by describing these fluxes first at the local instantaneous scale and then integrating over spatial and temporal distributions of soil saturation, precipitation, and wet environment evapotranspiration to calculate basin-wide climatic mean fluxes and soil saturation. The sensitivities of the mean fluxes are calculated by changing the mean precipitation and wet environment evapotranspiration. The model is applied to the Illinois River basin, and the impact of the basin's characteristics on the sensitivities is studied. For a relatively broad range of conditions the runoff processes tend to amplify climate change signals in precipitation and wet environment evapotranspiration, while evapotranspiration processes tend to dampen the same signals. These results indicate that it may be easier to detect climate changes in runoff measurements than in precipitation measurements.

Citation: Niemann, J. D., and E. A. B. Eltahir (2005), Sensitivity of regional hydrology to climate changes, with application to the Illinois River basin, *Water Resour. Res.*, *41*, W07014, doi:10.1029/2004WR003893.

1. Introduction

[2] An important issue in contemporary hydrology is the potential impact of climate changes on regional hydrologic fluxes. Many studies have investigated the impact of climate changes by calibrating complex numerical models to selected locations, varying the climatic inputs, and observing the resulting changes in runoff. Other studies have coupled descriptions of surface hydrology directly with global climate models to determine potential impacts. The difficulty in applying any complicated model is adequately constraining the parameter values from data. Often a variety of parameter sets can reproduce the available observations, but each parameter set produces a different forecast for unobserved conditions [*Schulz and Beven*, 2003].

[3] Another common approach is the application of simple water balance models to gain a qualitative understanding of the processes that control the impacts. *Dooge* [1992] used such a method to assess the sensitivity of the climatic mean fluxes to changes in climate. The heart of Dooge's approach is the *Budyko* [1950] hypothesis that the long-term evapotranspiration efficiency, the ratio of evapotranspiration to potential evapotranspiration (PET), must depend on long-term climatic forcing, in particular the humidity index (the ratio of precipitation to PET). Several empirical relationships have been developed that quantify the Budyko hypothesis mainly using annual observations of precipitation, streamflow, and PET for selected regions [*Schreiber*, 1904; *Ol'dekop*, 1911; *Turc*, 1954; *Pike*, 1964; *Zhang et al.*, 2001]. In addition, *Milly* [1993] used a model with stochastic precipitation events and a constant PET rate to derive a relationship for the evapotranspiration efficiency that depends not only on the humidity index but also on the capacity of the soil to store water. *Milly* [1994] extended the model to include seasonality of precipitation and PET as well as stochastic variation in the storage capacity. Similarly, *Sankarasubramanian and Vogel* [2002] used the "abcd" model to derive an expression for evapotranspiration efficiency that depends on the humidity index as well as the ratio of precipitation to a parameter describing the upper bound for the sum of evapotranspiration and soil moisture storage. Using several such relationships, *Dooge* [1992] examined the sensitivity of runoff to climatic changes, where sensitivity was measured as the percent change in the runoff that results from a percent change in precipitation or PET. Dooge observed that the sensitivity is highest when the humidity index is small. Among the relationships for evapotranspiration efficiency that Dooge considered the *Ol'dekop* [1911] expression produces the highest sensitivities for humid regions, whereas the *Schreiber* [1904] expression produces the highest sensitivities for arid regions. Because of these differences, Dooge concluded that such empirical functions do not adequately constrain the sensitivity of runoff to climate changes and suggested the use of simple physically based models as the next step.

[4] *Schaake* [1990] used such a model to evaluate the sensitivity of the Southeastern United States to changes in precipitation and PET. This spatially lumped model

0043-1397/05/2004WR003893$09.00

describes the water balance of the region at a monthly timescale. Runoff is determined from an expression similar to the Natural Resources Conservation Service (NRCS) curve number method. Evapotranspiration depends linearly on the water stored in the region, reaching the PET rate when the storage reaches a maximum allowable storage capacity. Using this model, Schaake found that a 10% increase in precipitation causes 20 to 44% increases in runoff in the region. A 10% increase in PET causes a 10 to 22% decrease in runoff. *Dooge et al.* [1999] used a similar spatially lumped water balance model to investigate the roles that seasonal variability in precipitation and PET play in determining the sensitivity of runoff. Three hypothetical climates were considered: a nonseasonal climate where precipitation and PET are constant, a temperate climate where precipitation is constant and PET varies sinusoidally, and a tropical climate where PET is constant and precipitation occurs only during a wet season. They found that the sensitivity of runoff to precipitation decreases with increasing humidity index. The nature of this decrease depends on the nature of the seasonal variability. For example, longer dry seasons result in lower sensitivities for all values of the humidity index. *Entekhabi and Eagleson* [1991] used a model with spatial variability to examine the sensitivity of soil moisture to changes in the humidity index. For hypothetical conditions, they observed high sensitivities when the humidity index was near one, especially when the spatial variability within the region was small.

[5] Data analysis methods have also been used to estimate the sensitivity of regional runoff to climate changes. In this approach, data for precipitation, runoff, and other variables are collected typically at the annual timescale. Then, one examines how much the runoff deviates from its long-term average as precipitation or other variables deviate from their long-term averages. This approach assumes that the response of annual runoff to annual changes in climatic inputs is the same as the response of the long-term mean runoff to changes in the long-term mean climatic inputs. *Risbey and Entekhabi* [1996] compiled annual observations of precipitation, temperature, and runoff for the Sacramento Basin in California. The runoff was found to be relatively insensitive to temperature but quite sensitive to precipitation. For example, if the annual precipitation was 40% above its long-term average, then the annual runoff rose approximately 60% above its average. *Sankarasubramanian et al.* [2001] performed a similar analysis using observations throughout the conterminous United States. Their results indicate that runoff is most sensitive to precipitation in parts of Arizona, Florida, and a region stretching from South Dakota through Illinois to Ohio. Runoff is least sensitive in regions such as Montana and North Dakota where snowpack is important to the water balance.

[6] In this paper, we build on these results by examining the sensitivities of soil saturation (soil moisture divided by porosity), surface runoff, groundwater runoff, and evapotranspiration using a process-based probabilistic model. The model includes some aspects of spatial and temporal variability but still relies on relatively few parameters. The model was previously used to describe the annual water balance of the Illinois River basin, a tributary of the Mississippi River that drains 69,264 km^2 including much of the state of Illinois [*Niemann and Eltahir*, 2004]. In this paper, the model is extended to consider the climatic mean values and their sensitivities. We first examine the sensitivities for the Illinois basin and then evaluate the sensitivities for hypothetical regions that differ from Illinois in prescribed ways. The primary objective is to understand the qualitative behavior of the sensitivities and the roles played by the physical and statistical properties of the region.

2. Model Development

[7] The model development begins with simple descriptions of the hydrologic fluxes at the local spatial scale and instantaneous timescale for two types of points: recharge locations and discharge locations. Recharge locations have hydraulic gradients in the vadose zone that are oriented to allow infiltration and recharge. Discharge locations have hydraulic gradients that allow discharge from the groundwater to the surface [*Hubbert*, 1940; *Freeze and Cherry*, 1979]. *Salvucci and Entekhabi* [1995] found that intermediate locations can also occur where the net exchange between the unsaturated and saturated zones is zero. The extent of these areas is expected to be larger for shallower soils, more clay-rich soils, flatter topography, and more arid climates. Our descriptions of the local instantaneous fluxes depend on the precipitation, PET, and soil saturation, which are treated as random variables. The spatial mean fluxes are found by integrating the local instantaneous models over the spatial distributions of the random variables, and the spatial mean PET is related to the wet environment evapotranspiration (WEET) using the complementary relation hypothesis (see below). Then, the space-time mean fluxes are found by integrating over the joint temporal distribution of spatial mean precipitation and soil saturation and the joint temporal distribution of spatial mean WEET and soil saturation. The results of this integration are expressions of the basin-wide climatic mean fluxes in terms of physical parameters and the basin-wide climatic mean soil saturation. The mean soil saturation is found by satisfying the statistical equilibrium of the region's inflows and outflows. The remainder of section 2 describes the model development in more detail.

2.1. Local Instantaneous Fluxes

[8] A simple model for the local instantaneous infiltration rate F can be written

$$\begin{aligned} &\text{Recharge locations} && F = \alpha(1-s) + K_h \\ &\text{Discharge locations} && F = 0 \end{aligned} \tag{1}$$

where α is an infiltrability parameter that describes the augmentation of the infiltration rate when the soil is unsaturated, s is the soil saturation ($0 \leq s \leq 1$), and K_h is the saturated hydraulic conductivity. The infiltration rate is highest when the soil is dry because water can fill voids in the vadose zone. In addition, a pressure gradient may increase the infiltration rate. When the soil is saturated, infiltration occurs at a rate that equals the saturated hydraulic conductivity. At discharge locations, no infiltration occurs because the hydraulic gradient is oriented to permit groundwater runoff. Similar models for infiltration rate have been used previously [*Holtan*, 1965; *Entekhabi*

and Eagleson, 1991; *Rodriguez-Iturbe et al.*, 1999; *Niemann and Eltahir*, 2004]. *Dooge et al.* [1999] used a similar but nonlinear infiltration expression that can be derived from Richard's equation by assuming a constant diffusivity.

[9] The local instantaneous surface runoff rate R can be calculated from the difference between the precipitation rate P and the infiltration rate F if interception and snowpack are neglected:

$$R = \begin{cases} P - F & \text{if } P > F \\ 0 & \text{if } P \le F \end{cases} \tag{2}$$

Together, equations (1) and (2) suggest that runoff can occur either because the soil saturation is large or the soil permeability characteristics (α and K_h) are small. The first situation corresponds to Horton runoff [*Freeze*, 1974] and the second situation corresponds to Dunne runoff [*Hewlett*, 1961; *Hewlett and Hibbert*, 1965; *Dunne and Black*, 1970].

[10] The local instantaneous groundwater recharge G is described by the simple model:

$$\begin{array}{ll} \text{Recharge locations} & G = K_h s^{\gamma} \\ \text{Discharge locations} & G = 0 \end{array} \tag{3}$$

where γ is a parameter that depends on soil texture [*Campbell*, 1974; *Clapp and Hornberger*, 1978]. This model can be derived from Darcy's law if the elevation change dominates the hydraulic gradient and the *Campbell* [1974] formulation is used to describe the unsaturated hydraulic conductivity [*Dooge et al.*, 1999; *Rodriguez-Iturbe et al.*, 1999; *Niemann and Eltahir*, 2004].

[11] The local instantaneous evapotranspiration rate E is written

$$E = \begin{cases} E_p s/\beta & \text{if } 0 \le s < \beta \\ E_p & \text{if } \beta \le s \le 1 \end{cases} \tag{4}$$

where E_p is the PET rate and β is the soil saturation that separates moisture-limited and energy/transport-limited evapotranspiration conditions. If $s < \beta$, the evapotranspiration rate depends linearly on the soil saturation, so the evapotranspiration is moisture limited. If $s \ge \beta$, the evapotranspiration occurs at the potential rate and is therefore energy or transport limited. Similar models have been explored previously by numerous authors [*Lowry*, 1959; *Feddes et al.*, 1976; *Molz*, 1981; *Entekhabi and Eagleson*, 1989; *Rodriguez-Iturbe et al.*, 1999; *Dooge et al.*, 1999; *Niemann and Eltahir*, 2004].

2.2. Spatial Mean Fluxes

[12] P, E_p, and s are treated as random variables. For simplicity, the spatial variations of these variables are assumed to be independent of each other. Immediately after a precipitation event, the soil saturation may strongly depend on the precipitation pattern. However, for most points in time, soil saturation patterns depend primarily on soil properties and topography [*Western et al.*, 1998; *Cosh and Brutsaert*, 1999]. If the three random variables are assumed independent, then the spatial mean fluxes can be determined by integrating over each variable's probability density function (PDF). Fortunately, it is not necessary to specify the spatial PDF for E_p. The evapotranspiration rate depends linearly on E_p, which implies that the spatial mean evapotranspiration rate depends only on the spatial mean of E_p. However, the spatial PDFs for precipitation and soil saturation are required.

[13] The spatial PDF for precipitation f_P is described by a mixed exponential distribution [*Entekhabi and Eagleson*, 1989]:

$$f_P = (1-\mu)\delta(P) + \frac{\mu^2}{\overline{P}} e^{-\mu P/\overline{P}} \qquad 0 \le P < \infty \tag{5}$$

where μ is the fraction of the region receiving precipitation, $\delta(\cdot)$ is the dirac delta function, and $\overline{P}$ is the spatial mean precipitation including locations with zero precipitation. In our notation, a bar over a variable indicates the spatial mean value. The spatial PDF of soil saturation f_s obeys an Erlang distribution in Illinois [*Niemann and Eltahir*, 2004]:

$$f_s = \frac{k^k}{\overline{s}^k (k-1)!} s^{k-1} e^{-ks/\overline{s}} \qquad 0 \le s < \infty. \tag{6}$$

$\overline{s}$ is the spatial mean soil saturation, and $k \equiv (\overline{s}/\sigma_s)^2$, where σ_s is the spatial standard deviation of the soil saturation. *Niemann and Eltahir* [2004] showed that k remains approximately constant among the spatial distributions observed at different times, which implies that the spatial standard deviation of soil saturation increases nearly linearly with the spatial mean.

[14] The Erlang distribution allows $s > 1$. This portion of the distribution is interpreted as locations where water is standing or flowing on the land surface (e.g., streams). Such locations are important because they also roughly correspond to the groundwater discharge locations in the basin. When using the PDF in equation (6), values of $s > 1$ are replaced with $s = 1$, which is equivalent to replacing the portion of the distribution above one with a probability mass at $s = 1$. In addition, this portion of the distribution is used to represent the discharge locations in equations (1) and (3).

[15] After integrating over the spatial PDFs, the following analytical expressions are determined for the spatial mean surface runoff $\overline{R}$, groundwater recharge $\overline{G}$, and evapotranspiration $\overline{E}$:

$$\overline{R} = \overline{P}(k/\overline{s})^k \left\{ \frac{e^{-(K_h+\alpha)/i}}{(k/\overline{s} - \alpha/i)^k} + \sum_{j=0}^{k-1} \frac{e^{-k/\overline{s}}}{(k-1-j)!} \cdot \left[(\overline{s}/k)^{j+1} - \frac{e^{-K_h/i}}{(k/\overline{s} - \alpha/i)^{j+1}} \right] \right\} \tag{7}$$

$$\overline{G} = K_h \frac{(k-1+\gamma)!}{(k-1)!} (k/\overline{s})^{-\gamma} \left[1 - e^{-k/\overline{s}} \sum_{j=0}^{k-1+\gamma} \frac{(k/\overline{s})^{k-1+\gamma-j}}{(k-1+\gamma-j)!} \right] \tag{8}$$

$$\overline{E} = \overline{E}_p \left[\frac{\overline{s}}{\beta} - \sum_{j=1}^{k} \frac{j(k/\overline{s})^{k-1-j} \beta^{k-1-j} e^{-k\beta/\overline{s}}}{(k-j)!} \right] \tag{9}$$

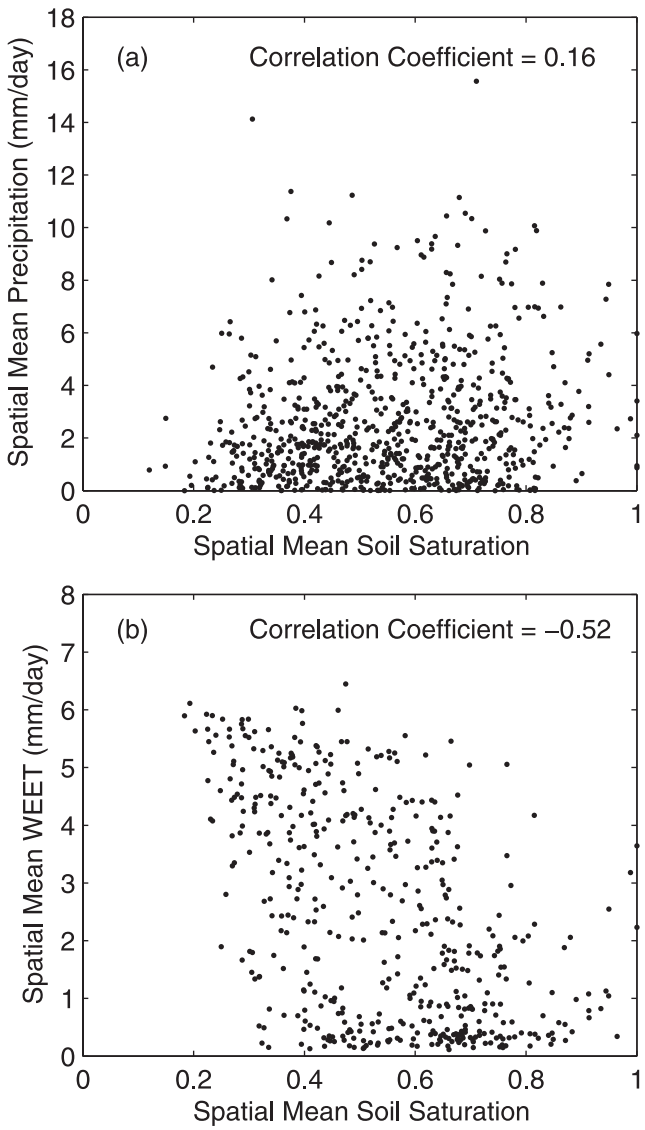

Figure 1. (a) The dependence of the spatial mean precipitation $\overline{P}$ on the spatial mean soil saturation $\overline{s}$ and (b) the dependence of the spatial mean WEET $\overline{E}_w$ on the spatial mean soil saturation $\overline{s}$.

where i is the spatial mean precipitation rate among locations where the precipitation rate is nonzero. This quantity has been found to remain relatively constant for a given region [*Eltahir and Bras*, 1993].

[16] Observations suggest that the PET rate is itself a function of the evapotranspiration rate in a region [*Bouchet*, 1963; *Brutsaert and Strickler*, 1979; *Hobbins et al.*, 2001a, 2001b]. When the evapotranspiration rate is reduced due to a lack of moisture, the available energy is used instead to increase the air temperature and humidity gradient, which increases the PET. *Hobbins et al.* [2001a, 2001b] argue that a complementary relationship of the form $\overline{E} + \overline{E}_p = 2\overline{E}_w$ describes this interdependence. In this expression, $\overline{E}_w$ is the wet environment evapotranspiration rate (WEET), which is the PET for the region if moisture were unlimited. Notice that we write the complementary relationship with the spatial means because the process described above occurs at a regional rather than local scale. This approach allows local evapotranspiration rates to occur up to the PET rate, which may exceed the WEET rate. We can easily rewrite equation (9) in terms of $\overline{E}_w$ instead of $\overline{E}_p$. Notice that equation (9) can be written as $\overline{E} = \overline{E}_p\overline{\varepsilon}$, where $\overline{\varepsilon}$ is an evapotranspiration efficiency, which corresponds to the term in the square brackets. Using the complementary relationship, any evapotranspiration model with this form can be rewritten $\overline{E} = \overline{E}_w 2\overline{\varepsilon}/(1+\overline{\varepsilon})$. This modified expression for evapotranspiration is preferred for our purposes because $\overline{E}_w$ is less dependent on the regional hydrology than $\overline{E}_p$.

2.3. Space-Time Mean Fluxes

[17] We now turn to the calculation of the space-time mean fluxes for the region. The spatial mean fluxes depend on three random variables $\overline{P}$, $\overline{E}_w$, and $\overline{s}$, which can vary in time. If the temporal variations of these variables were assumed to be independent of each other, we could simply integrate over their individual PDFs. This approach was used in the previous section to calculate the spatial means analytically. To calculate the space-time means, we generalize the procedure to consider correlation between the variables. Temporal correlations may significantly alter the regional water balance. For example, *Wolock and McCabe* [1999] found that the relative timing of precipitation and PET during the year play a significant role in determining the evapotranspiration efficiency. If the PET is largest during the dry season, then the efficiency is reduced due to the lack of available water. The ability of the soil to store water between seasons is an important moderator of this impact [*Milly*, 1994; *Sankarasubramanian and Vogel*, 2002].

[18] The correlation between $\overline{P}$ and $\overline{s}$ and the correlation between $\overline{E}_w$ and $\overline{s}$ are shown in Figure 1. To generate Figure 1, the spatial mean precipitation rate was determined for the Illinois basin using 71 gages from the National Climatic Data Center, and the spatial mean soil saturation was found from measurements at 19 locations [*Hollinger and Isard*, 1994]. Because of data limitations, the spatial mean WEET was determined from 4 locations using a standard method based on the Priestley-Taylor equation [*Shuttleworth*, 1993; *Hobbins et al.*, 2004]. All means were determined using the well-known Thiessen polygon method. The correlation coefficient for $\overline{P}$ and $\overline{s}$ is quite small and positive (0.16), whereas the correlation coefficient for $\overline{E}_w$ and $\overline{s}$ is more substantial but negative (−0.52). The lower correlation between $\overline{P}$ and $\overline{s}$ is expected because the spatial mean precipitation is highly variable in time, whereas the spatial mean soil saturation is less erratic.

[19] With these observations in hand, the space-time mean surface runoff $E[\overline{R}]$ can be found. In our notation, $E[\cdot]$ denotes the temporal or climatic mean. $\overline{R}$ depends on two random variables $\overline{P}$ and $\overline{s}$, so $E[\overline{R}]$ can be determined from

$$E[\overline{R}] = \int_{\overline{s}=0}^{1}\int_{\overline{P}=0}^{\infty} \overline{R} f_{\overline{s},\overline{P}} d\overline{s} d\overline{P} \tag{10}$$

where $f_{\overline{s},\overline{P}}$ is the joint distribution of $\overline{s}$ and $\overline{P}$. One can rewrite this expression as

$$E[\overline{R}] = \int_{\overline{s}=0}^{1}\int_{\overline{P}=0}^{\infty} \overline{P} f_{\overline{P}|\overline{s}} d\overline{P} \overline{r}_c(\overline{s}) f_{\overline{s}} d\overline{s} \tag{11}$$

where $f_{\overline{P}|\overline{s}}$ is the temporal distribution of $\overline{P}$ for a given $\overline{s}$, $f_{\overline{s}}$ is the temporal distribution of $\overline{s}$, and $\overline{r}_c(\overline{s})$ is the spatial mean surface runoff coefficient ($\overline{r}_c(\overline{s}) \equiv \overline{R}/\overline{P}$, which is known from equation (7)). The integration over $\overline{P}$ simply produces the space-time mean precipitation for a given spatial mean soil saturation $E[\overline{P}|\overline{s}]$, so equation (11) becomes

$$E[\overline{R}] = \int_{\overline{s}=0}^{1} E[\overline{P}|\overline{s}]\overline{r}_c(\overline{s})f_{\overline{s}}d\overline{s}. \quad (12)$$

The conditional mean can be determined from

$$E[\overline{P}|\overline{s}] = E[\overline{P}] + \rho_{\overline{P},\overline{s}}(\sigma_{\overline{P}}/\sigma_{\overline{s}})(\overline{s} - E[\overline{s}]) \quad (13)$$

where $E[\overline{P}]$ is the space-time mean precipitation, $E[\overline{s}]$ is the space-time mean soil saturation, $\rho_{\overline{P},\overline{s}}$ is the correlation between $\overline{P}$ and $\overline{s}$ ($\rho_{\overline{P},\overline{s}} = 0.16$ from Figure 1), $\sigma_{\overline{P}}$ is the temporal standard deviation of $\overline{P}$, and $\sigma_{\overline{s}}$ is the temporal standard deviation of $\overline{s}$. Substituting this expression for the conditional mean into equation (12), one obtains

$$E[\overline{R}] = \int_{\overline{s}=0}^{1} \left\{E[\overline{P}] + \rho_{\overline{P},\overline{s}}(\sigma_{\overline{P}}/\sigma_{\overline{s}})(\overline{s} - E[\overline{s}])\right\}\overline{r}_c(\overline{s})f_{\overline{s}}d\overline{s}. \quad (14)$$

If $f_{\overline{s}}$ is known, this relationship can be used to find the space-time mean runoff for a given space-time mean precipitation and soil saturation.

[20] Similar expressions can be derived for groundwater recharge and evapotranspiration. The expression for groundwater recharge depends on only one random variable ($\overline{s}$), so the issue of correlation between random variables is not relevant. The space-time mean recharge $E[\overline{G}]$ is simply

$$E[\overline{G}] = \int_{\overline{s}=0}^{1} K_h\overline{G}(\overline{s})f_{\overline{s}}d\overline{s}. \quad (15)$$

The evapotranspiration is similar to the surface runoff because it depends on two random variables ($\overline{E}_w$ and $\overline{s}$), so their correlation should be considered. One can find an expression for the space-time mean evapotranspiration $E[\overline{E}]$ from the same approach used for the surface runoff. The resulting expression is

$$E[\overline{E}] = \int_{\overline{s}=0}^{1} \left\{E[\overline{E}_w] + \rho_{\overline{E}_w,\overline{s}}\left(\sigma_{\overline{E}_w}/\sigma_{\overline{s}}\right)(\overline{s} - E[\overline{s}])\right\} \cdot 2\overline{\varepsilon}(\overline{s})/\{1 + \overline{\varepsilon}(\overline{s})\}f_{\overline{s}}d\overline{s} \quad (16)$$

where $E[\overline{E}_w]$ is the space-time mean WEET, $\rho_{\overline{E}_w,\overline{s}}$ is the correlation between $\overline{E}_w$ and $\overline{s}$ ($\rho_{\overline{E}_w,\overline{s}} = -0.52$ from Figure 1), and $\sigma_{\overline{E}_w}$ is the temporal standard deviation of $\overline{E}_w$. Similarly, one can calculate the space-time mean potential evapotranspiration $E[\overline{E}_p]$ from

$$E[\overline{E}_p] = \int_{\overline{s}=0}^{1} \left\{E[\overline{E}_w] + \rho_{\overline{E}_w,\overline{s}}\left(\sigma_{\overline{E}_w}/\sigma_{\overline{s}}\right)(\overline{s} - E[\overline{s}])\right\} \cdot 2/\{1 + \overline{\varepsilon}(\overline{s})\}f_{\overline{s}}d\overline{s}. \quad (17)$$

[21] In order to evaluate the integrals in equations (14) to (17), one must determine the form of the temporal distribution of $\overline{s}$. *Niemann and Eltahir* [2004] found that the temporal variability within a given year obeys a beta distribution, so it is reasonable to hypothesize that the total temporal variability of $\overline{s}$ also conforms to a beta distribution. The beta distribution depends on two parameters that can be specified if the mean $E[\overline{s}]$ and standard deviation $\sigma_{\overline{s}}$ are known. The compatibility of the data and the beta distribution can be evaluated quantitatively using the Kolmogorov-Smirnov (KS) test, which compares the maximum observed deviation between the two distributions with the deviation expected at a given level of probability [*Tadikamalla*, 1990; *Bain and Engelhardt*, 1992]. The beta distribution model passes the KS test at the 20% probability level, so we conclude that the beta distribution is an adequate model of the temporal variability.

[22] In order to use the beta distribution to represent the variability of $\overline{s}$ for different climatic states, one must understand how $\sigma_{\overline{s}}$ behaves as $E[\overline{s}]$ changes. Unfortunately, no observations are available to describe the variability of $\overline{s}$ in the Illinois basin for different climatic states. To overcome this limitation, we assume that the behavior of the climatic standard deviation for different climatic means is the same as the behavior of the annual (i.e., within year) standard deviation for different annual means. Such an assumption is justified if the within-year variation of $\overline{s}$ comprises much more of the total temporal variation than the interannual variability. Using the soil saturation observations from Illinois, we find that the average standard deviation for temporal variability within a year is $\sigma_{\overline{s}} = 0.162$ and the total temporal standard deviation is $\sigma_{\overline{s}} = 0.173$. Thus the within-year variability dominates the total variability. *Niemann and Eltahir* [2004] found that the annual standard deviation remains relatively constant between years, so we will also assume that the climatic standard deviation remains constant for different climatic means.

[23] Figure 2 shows the space-time mean surface runoff coefficient $E[\overline{r}_c] \equiv E[\overline{R}]/E[\overline{P}]$, recharge efficiency $E[\overline{g}] \equiv E[\overline{G}]/K_h$, and relative evapotranspiration $E[\overline{\eta}] \equiv E[\overline{E}]/E[\overline{E}_w]$ as determined from the model. Aside from the statistical parameters, the space-time mean surface runoff coefficient depends only on α/i, K_h/i, and $E[\overline{s}]$. The space-time mean groundwater efficiency depends only on γ and $E[\overline{s}]$, and relative evapotranspiration depends only on β and $E[\overline{s}]$. For comparison, the dotted contours in Figure 2 show the same quantities if the correlations $\rho_{\overline{P},\overline{s}}$ and $\rho_{\overline{E}_w,\overline{s}}$ are neglected. The correlations result in higher surface runoff coefficients and lower relative evapotranspirations. The positive correlation between $\overline{s}$ and $\overline{P}$ suggests that the soil tends to be wetter when precipitation occurs. Thus the correlation promotes the occurrence of Dunne runoff. Similarly, the negative correlation between $\overline{s}$ and $\overline{E}_w$ implies that soil moisture is often limited when the WEET rates are high. As a result, the relative evapotranspiration is reduced. The impacts of the correlations are most pronounced when $E[\overline{s}]$ is small and α/i and β are large. Under these conditions the correlations can adjust the surface runoff coefficient and relative evapotranspiration by more than 40%. For conditions that are more representative of the Illinois basin (see parameters in Table 1), the correlation impacts are less than 10%.

2.4. Statistical Equilibrium

[24] Figure 2b allows us to determine the space-time mean groundwater recharge if $E[\overline{s}]$ is known, but we would also like to know the space-time mean groundwater runoff.

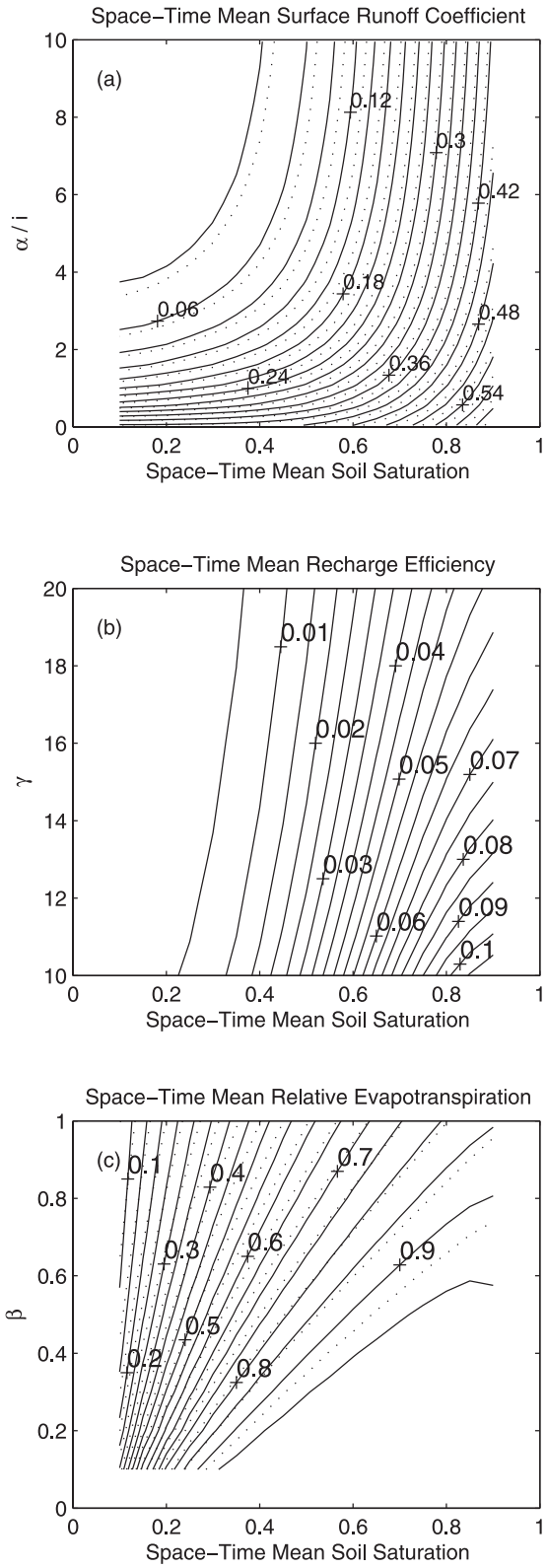

Figure 2. Contour plots of modeled space-time mean (a) surface runoff coefficient $E[\overline{r}_c]$, (b) recharge efficiency $E[\overline{g}]$, and (c) relative evapotranspiration $E[\overline{\eta}]$.

This variable can be found by assuming that the groundwater reservoir exhibits a statistical equilibrium at the climatic timescale. Such an equilibrium condition is valid if the climate is in a stationary state and implies that the mean groundwater inflow equals the mean groundwater outflow. If the only fluxes entering and exiting the groundwater reservoir are recharge and runoff, then the space-time mean groundwater recharge must equal the space-time mean groundwater runoff. As a result, Figure 2b describes both the groundwater recharge and runoff. Notice that we have neglected subsurface transfer of water across the region boundary and evapotranspiration from the groundwater, which are potentially important during the summer months [*Yeh*, 2003].

[25] Although Figure 2 can now be used to find all of the space-time mean hydrologic fluxes for a given $E[\overline{s}]$, we would still like to infer $E[\overline{s}]$ from $E[\overline{P}]$ and $E[\overline{E}_w]$. This task can be accomplished by considering another statistical equilibrium condition. If the climate is in a stationary state, the mean input of water into the region must balance the mean output of water. Mathematically, this implies

$$E[\overline{P}] = E[\overline{R}] + E[\overline{G}] + E[\overline{E}] \tag{18}$$

where we are using $E[\overline{G}]$ to represent the groundwater runoff. This expression can be written as

$$E[\overline{P}] = E[\overline{r}_c]E[\overline{P}] + E[\overline{g}]K_h + E[\overline{\eta}]E[\overline{E}_w]. \tag{19}$$

Notice that $E[\overline{r}_c]$, $E[\overline{g}]$, and $E[\overline{\eta}]$ are all monotonic functions of $E[\overline{s}]$ (Figure 2), so only one $E[\overline{s}]$ value satisfies this equation if all other values are known. Thus the expression can be used to determine $E[\overline{s}]$ for given values of $E[\overline{P}]$ and $E[\overline{E}_w]$. *Entekhabi and Eagleson* [1991] used a similar statistical equilibrium condition in their analysis.

3. Model Application

[26] In order to apply the model, appropriate values must be determined for the model parameters (α, i, K_h, β, and γ). *Niemann and Eltahir* [2004] developed a calibration method for the model at the annual timescale. In that procedure, the space-time mean fluxes were calculated individually from observations of $E[\overline{s}]$ and trial values of the parameters. The trial parameters were constrained to fall within reasonable ranges as determined from independent information about the Illinois basin. The parameter values that minimized the disagreement between the model predictions and observations of $E[\overline{E}]$ and $E[\overline{Q}] \equiv E[\overline{R}] + E[\overline{G}]$ were selected. The model was then verified using $E[\overline{P}]$ and $E[\overline{E}_p]$ data and the statistical equilibrium condition in equation (18) to infer the value of $E[\overline{s}]$ and the associated mean fluxes. These fluxes were then compared with observations.

[27] The parameter values determined by *Niemann and Eltahir* [2004] are applicable at both the annual and climatic timescales because they represent physical characteristics of the region. However, *Niemann and Eltahir* [2004] estimated the parameter values to optimize the results when all correlations were neglected and PET observations were used instead of WEET estimates. As a result, we recalibrated the model at the annual timescale when the appropriate correlations between $\overline{P}$ and $\overline{s}$ and $\overline{E}_w$ and $\overline{s}$ were included. The revised calibration produces slightly different parameter values (Table 1), but the model results at the annual timescale are visually identical to those presented

Table 1. Parameters Determined for the Illinois Basin When Correlations Are Neglected and PET Is Used and When Correlations Are Included and WEET Is Used[a]

Correlations Neglected and PET Used	Correlations Included and WEET Used
Calibrated Parameters	
$K_h = 2.86 \times 10^{-5}$ cm/s = 9 m/yr	$K_h = 2.86 \times 10^{-5}$ cm/s = 9 m/yr
$\alpha = 9.5 \times 10^{-5}$ cm/s = 30 m/yr	$\alpha = 10.5 \times 10^{-5}$ cm/s = 33 m/yr
$\beta = 0.87$	$\beta = 0.91$
$\gamma = 19$	$\gamma = 19$
Observed/Fixed Characteristics	
$k = 11$	$\sigma_{\overline{s}} = 0.17$
$i = 3.17 \times 10^{-5}$ cm/s = 10 m/yr	$\rho_{\overline{P},\overline{s}} = 0.16$
$E[\overline{P}] = 0.921$ m/yr	$\rho_{\overline{E}_w,\overline{s}} = -0.52$
$E[\overline{E}_w] = 0.877$ m/yr	$\sigma_{\overline{P}} = 0.86$ m/yr
	$\sigma_{\overline{E}_w} = 0.68$ m/yr

[a]The former parameters are equivalent to those of *Niemann and Eltahir* [2004].

previously. Thus we refer the reader to *Niemann and Eltahir* [2004] for more information about the model calibration.

[28] Once the model parameters values have been specified, the model can be applied and its results compared to those obtained from empirical equations for space-time mean evapotranspiration efficiency $E[\overline{\varepsilon}] \equiv E[\overline{E}]/E[\overline{E}_p]$ [*Schreiber*, 1904; *Ol'dekop*, 1911; *Turc*, 1954; *Pike*, 1964; *Zhang et al.*, 2001]. Although such expressions are usually written to find $E[\overline{\varepsilon}]$, they can be rearranged to determine the space-time mean runoff coefficient $E[\overline{q}_c] \equiv E[\overline{Q}]/E[\overline{P}]$ where $E[\overline{Q}]$ is the space-time mean runoff (including surface and groundwater runoff). In particular, one can obtain

$$\begin{aligned} &\text{Turc-Pike} && E[\overline{q}_c] = 1 - \frac{1}{\sqrt{1 + D_E^2}} \\ &\text{Ol'dekop} && E[\overline{q}_c] = 1 - \frac{1}{D_E}\tanh D_E \\ &\text{Schreiber} && E[\overline{q}_c] = \exp(-1/D_E) \end{aligned} \tag{20}$$

where D_E is the humidity index $D_E \equiv E[\overline{P}]/E[\overline{E}_p]$. Similarly for short grass or crops (which is appropriate for Illinois), the *Zhang et al.* [2001] expression implies:

$$E[\overline{q}_c] = 1 - \frac{1}{D_E}\left[\frac{1 + 0.5/D_E}{1 + 1/D_E + 0.5/D_E^2}\right] \tag{21}$$

[29] Unlike the empirical expressions, the model does not depend simply on the ratio of the space-time mean precipitation to PET; it depends on their individual values. Thus it does not produce a unique relationship between $E[\overline{q}_c]$ and D_E. Figure 3a plots two curves for the model along with the empirical expressions for $E[\overline{q}_c]$. One curve was produced by fixing the precipitation at the observed value for the Illinois basin ($E[\overline{P}] = 0.921$ m/yr) and varying the WEET to produce a range of D_E values. The other curve was produced by fixing the WEET at the observed value ($E[\overline{E}_w] = 0.877$ m/yr) and varying the precipitation. Two important results are visible in Figure 3a. First, the model produces relationships between D_E and $E[\overline{q}_c]$ that have the same general form as the empirical relationships. In particular, the model results closely resemble the *Zhang et al.* [2001] curve from equation (21), which has a similar shape to the Schreiber curve (not shown). This observation confirms that the model produces realistic runoff coefficients for a range of D_E values. Second, the model produces similar relationships for $E[\overline{q}_c]$ irrespective of whether $E[\overline{P}]$ or $E[\overline{E}_w]$ was varied to produce the range of D_E. This

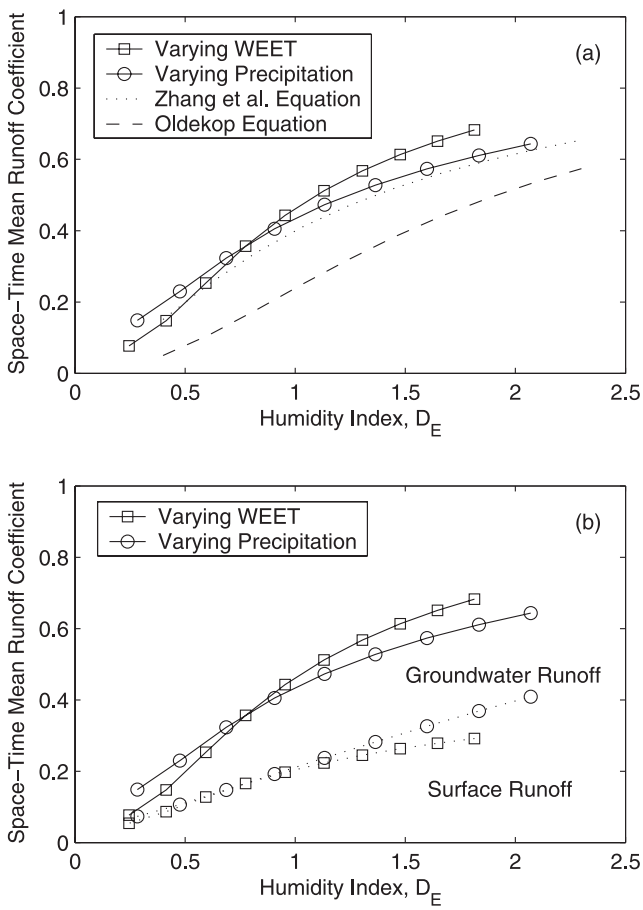

Figure 3. Analysis of space-time mean runoff coefficient $E[\overline{q}_c]$. (a) Comparison of $E[\overline{q}_c]$ from the probabilistic model to two empirical relationships. (b) Contributions of surface and groundwater runoff to the runoff coefficients from the model.

observation can be interpreted by rewriting the statistical equilibrium condition (equation (18)) in terms of $E[\overline{r}_c]$, $E[\overline{g}]$, and $E[\overline{\eta}]$. One can show that the equilibrium condition requires

$$1 = E[\overline{r}_c] + E[\overline{g}]/D_{K_h} + E[\overline{\eta}]/D_{E_w} \quad (22)$$

where $D_{K_h} \equiv E[\overline{P}]/K_h$ and $D_{E_w} \equiv E[\overline{P}]/E[\overline{E}_w]$, which are two new humidity indices. The terms $E[\overline{r}_c]$, $E[\overline{g}]$, and $E[\overline{\eta}]$ in the model all depend on $E[\overline{s}]$, which is determined from this expression. Thus equation (22) states that the model's dependence on space-time mean precipitation and WEET can be recast as a dependence on two humidity indices D_{E_w} and D_{K_h}. When $E[\overline{E}_w]$ was varied to produce a curve for Figure 3a, only D_{E_w} changed. When $E[\overline{P}]$ was varied, both humidity indices changed simultaneously. The difference between the two curves gives an indication of the influence of D_{K_h} on the model results. Because the two curves are so similar, one concludes that D_{E_w} has a much stronger influence on the runoff coefficient than D_{K_h}, which is consistent with the fact that the empirical equations for runoff coefficient and evapotranspiration efficiency have traditionally been written only in terms of D_E, which is similar to D_{E_w}. The presence of D_{K_h} in the model is similar to the results of *Milly* [1993, 1994] and *Sankarasubramanian and Vogel* [2002], who derived a dependence on the storage capacity of the region. In the present case, the second index describes a capacity for water movement at saturation rather than a storage capacity.

[30] The model also provides insight into the physical origin of the empirical expressions for evapotranspiration efficiency and runoff coefficient. Numerous authors [e.g., *Milly*, 1994; *Zhang et al.*, 2001; *Sankarasubramanian and Vogel*, 2002] have suggested that the empirical expressions for evapotranspiration efficiency describe the transition between moisture-limited conditions and energy-limited conditions. When moisture is limited, an approximate maximum for $E[\overline{E}]$ is $E[\overline{P}]$. When moisture is unlimited, an approximate maximum for $E[\overline{E}]$ is $E[\overline{E}_p]$. These limiting conditions on evapotranspiration also imply low runoff coefficients when evapotranspiration is moisture limited (small values of D_E), and larger runoff coefficients when evapotranspiration is limited by its potential rate (large values of D_E). Such changes in the runoff coefficient must be accommodated by changes in the production of surface and/or groundwater runoff. The dashed lines in Figure 3b show the space-time mean surface runoff coefficient $E[\overline{r}_c]$ as $E[\overline{P}]$ or $E[\overline{E}_w]$ is varied to produce the variation in D_E. Thus the area below the dashed lines represents the contribution from surface runoff, and the area above the dashed lines and below the solid lines represents the contribution from groundwater runoff. The surface runoff coefficient lines are approximately linear, particularly when $E[\overline{P}]$ is varied. The surface runoff coefficient increases with D_E because a higher D_E value results in a higher $E[\overline{s}]$ value, which improves the efficiency of surface runoff production for a given precipitation. The approximate linearity of the surface runoff coefficient lines suggests that the curvature of the empirical $E[\overline{q}_c]$ equations, which is caused by the evapotranspiration limits described earlier, is accommodated by nonlinear variations in the contribution of groundwater.

[31] Understanding the model's relationships between $E[\overline{P}]$ and $E[\overline{s}]$, $E[\overline{R}]$, $E[\overline{G}]$, and $E[\overline{E}]$ will be helpful in interpreting the sensitivity results that are described later in this paper. Figure 4a shows that the relationship between $E[\overline{P}]$ and $E[\overline{s}]$ is approximately linear within the range examined, although a slight decrease in slope is observed at higher values of the precipitation. The near linearity is helpful in interpreting the behavior of the hydrologic system because it allows us to interpret changes in precipitation as proxies for changes in soil saturation. Figure 4b shows a concave-up relationship between $E[\overline{P}]$ and $E[\overline{R}]$. This shape is not surprising because an increase in precipitation results in an increase in soil saturation, which promotes Dunne runoff. Figure 4c shows that the relationship between $E[\overline{P}]$ and $E[\overline{G}]$ is a portion of an S-shaped curve. As precipitation increases, the soil moisture also increases, which implies that groundwater recharge becomes more efficient. The increasing efficiency causes the concave-up portion of the groundwater runoff curves. As the precipitation increases further, a larger portion of the basin is occupied by groundwater discharge points, which limits the number of recharge locations. This limitation restricts the increase of the groundwater runoff coefficient and produces the convex-up portion of the curve. Figure 4d shows the relationship between $E[\overline{P}]$ and $E[\overline{E}]$, which is convex up. When precipitation is low, the slope of the curve is large because most of the evapotranspiration is moisture limited and thus dependent on the soil saturation value induced by the precipitation. When precipitation is large, the slope reduces because more points are energy limited and therefore independent of the soil saturation.

4. Sensitivity to Climate Change

[32] For the purposes of this paper, climate changes are expressed as changes in the space-time means of precipitation and WEET. By perturbing WEET instead of PET, we are evaluating the sensitivity to a variable that is less dependent on the regional hydrology. We focus on the sensitivity of four space-time mean components of the water balance: soil saturation, surface runoff, groundwater runoff, and evapotranspiration. Our definition of sensitivity is the percent change in a hydrologic variable that results from a percent change in precipitation or WEET, which is similar to the definition introduced by *Schaake* [1990] and used by *Dooge* [1992]. For example, the sensitivity of soil moisture to precipitation is denoted as $\Upsilon_{E[\overline{s}],E[\overline{P}]}$ and can be written

$$\Upsilon_{E[\overline{s}],E[\overline{P}]} \equiv \frac{\Delta E[\overline{s}]/E[\overline{s}]}{\Delta E[\overline{P}]/E[\overline{P}]} \quad (23)$$

where $E[\overline{s}]$ and $E[\overline{P}]$ are the soil saturation and precipitation for the current climate, $\Delta E[\overline{P}]$ is a small perturbation from the current precipitation, and $\Delta E[\overline{s}]$ is the resulting change in the soil saturation, which can be calculated numerically. *Schaake* [1990] refers to this quantity as an elasticity, a term borrowed from economics. If the sensitivity is above one, the variable is considered elastic because it exhibits an augmented response to a change in the perturbed quantity. If the sensitivity is below one, the variable is inelastic because

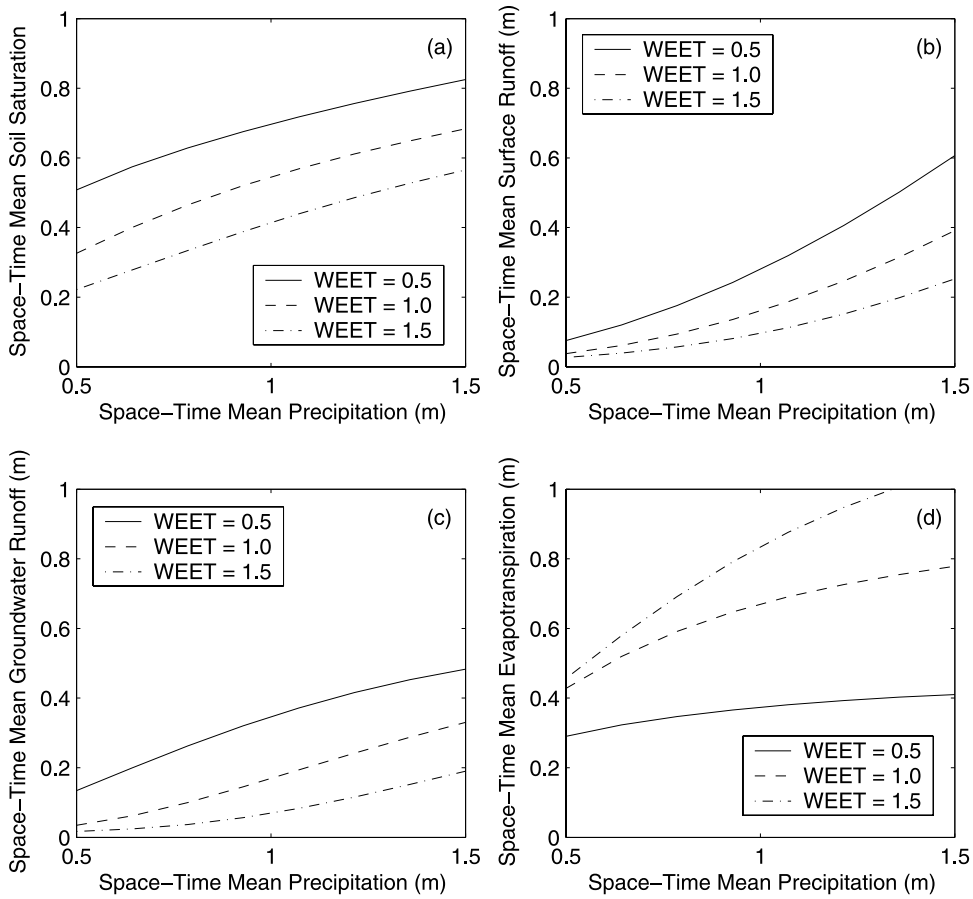

Figure 4. Behavior of the space-time mean (a) soil saturation $E[\overline{s}]$, (b) surface runoff $E[\overline{R}]$, (c) groundwater runoff $E[\overline{G}]$, and (d) evapotranspiration $E[\overline{E}]$ as a function of mean precipitation $E[\overline{P}]$ and WEET $E[\overline{E}_w]$.

it has a dampened response to the change. Notice that the means considered here are long-term or climatic means, which include some elements of interannual variability. Previous studies of the sensitivities have not included interannual variability.

[33] Figure 5 shows the sensitivities of the soil saturation, surface runoff, groundwater runoff, and evapotranspiration to changes in precipitation (i.e., $\Upsilon_{E[\overline{s}],E[\overline{P}]}$, $\Upsilon_{E[\overline{R}],E[\overline{P}]}$, $\Upsilon_{E[\overline{G}],E[\overline{P}]}$, and $\Upsilon_{E[\overline{E}],E[\overline{P}]}$). To calculate these sensitivities, all the physical and statistical characteristics determined for the Illinois basin were used except for $E[\overline{P}]$ and $E[\overline{E}_w]$, which were varied as shown by the coordinate axes. Thus a single point in each plot, which is labeled, corresponds to the current climate of the Illinois basin, and the other points represent hypothetical regions that differ from Illinois only in their precipitation and WEET. By plotting the sensitivities in this fashion, one can estimate the sensitivities for the Illinois basin and study how the sensitivities change with $E[\overline{P}]$ and $E[\overline{E}_w]$.

[34] The sensitivity of soil moisture has contours that are approximately radial from the origin (Figure 5a). The radial pattern indicates that the sensitivity is relatively well described by a function of D_{E_w}. In other words, the individual values of the precipitation and WEET have only a weak influence on the model's sensitivity. The point in the plot that describes the current climate of the Illinois basin suggests that a 1% increase in precipitation would result in less than a 1% increase in soil saturation. In fact, no combination of precipitation and WEET shown in the plot results in a 1% or larger increase in soil saturation. This behavior implies that the hydrologic system does not need a full 1% increase in soil saturation to produce outflows that balance the increase in the inflow. The highest sensitivities in Figure 5a are observed for hypothetical regions with low $E[\overline{P}]$ and high $E[\overline{E}_w]$. This result can be interpreted by rewriting equation (23) as follows:

$$\Upsilon_{E[\overline{s}],E[\overline{P}]} = \frac{\Delta E[\overline{s}]}{\Delta E[\overline{P}]}\frac{E[\overline{P}]}{E[\overline{s}]} \approx \frac{\partial E[\overline{s}]}{\partial E[\overline{P}]}\frac{E[\overline{P}]}{E[\overline{s}]}. \tag{24}$$

The partial derivative is equivalent to the slopes of the curves in Figure 4a, which are largest for small precipitation values. This observation suggests that the system must adjust its state variable more to account for changes in precipitation when precipitation is small. Figure 4a also shows that the ratio of precipitation to soil saturation is larger when the WEET is large. As a result, the sensitivity of the soil saturation to precipitation in regions with high WEET is further augmented.

[35] Figure 5b shows the sensitivity of surface runoff to precipitation $\Upsilon_{E[\overline{R}],E[\overline{P}]}$. Figure 5b has a very different

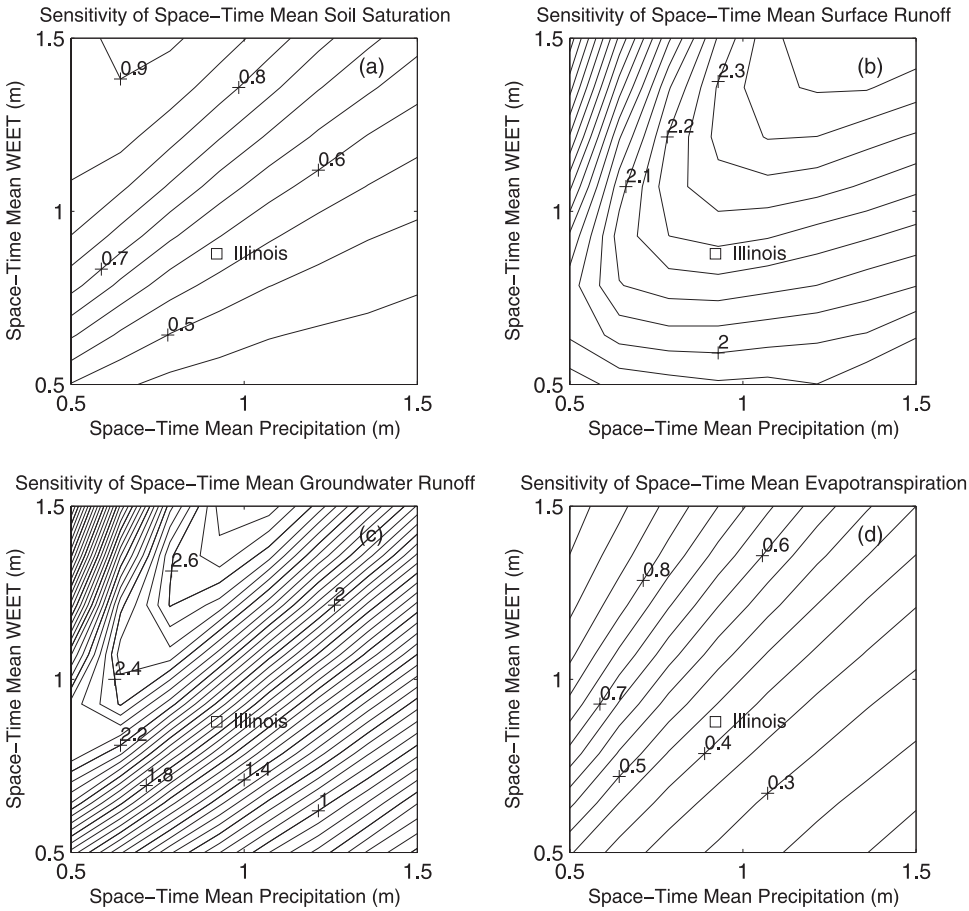

Figure 5. The sensitivities of hydrologic variables to precipitation. (a) Sensitivity of soil saturation $\Upsilon_{E[\bar{s}],E[\bar{P}]}$, (b) sensitivity of surface runoff $\Upsilon_{E[\bar{R}],E[\bar{P}]}$, (c) sensitivity of groundwater runoff $\Upsilon_{E[\bar{G}],E[\bar{P}]}$, and (d) sensitivity of evapotranspiration $\Upsilon_{E[\bar{E}],E[\bar{P}]}$. All of these plots show contours of their associated sensitivity.

pattern than Figure 5a, which implies that the sensitivity of surface runoff does not depend primarily on D_{E_w}. The sensitivity for the Illinois basin is near 2.2, and the sensitivity for the entire range of hypothetical climates considered is well above 1. This result is important because it suggests that changes in precipitation will be exaggerated in the surface runoff. The reason for these high sensitivities can be seen in Figure 4b. Notice that $\Upsilon_{E[\bar{R}],E[\bar{P}]}$ can be approximated

$$\Upsilon_{E[\bar{R}],E[\bar{P}]} \approx \frac{\partial E[\bar{R}]}{\partial E[\bar{P}]} \frac{E[\bar{P}]}{E[\bar{R}]} = \frac{\partial E[\bar{R}]}{\partial E[\bar{P}]} / E[\bar{r}_c]. \tag{25}$$

We expect higher sensitivities for large precipitation values because of the emergence of Dunne runoff shown in Figure 4b. In addition, the sensitivities are larger when WEET is large because the runoff coefficient is smaller due to the strength of the evapotranspiration process.

[36] Figure 5c shows the sensitivity of groundwater runoff to precipitation $\Upsilon_{E[\bar{G}],E[\bar{P}]}$. Figure 5c shows that the sensitivity is typically greater than one, but it can be less than one for regions with large precipitation and small WEET. For the Illinois basin the sensitivity is about 1.9. The wide range in sensitivity values suggests that small errors in the estimates of precipitation and WEET will result in relatively large changes in the estimated sensitivity. Thus the plot implies that the sensitivity of groundwater runoff may be the most difficult sensitivity to predict accurately. The highest sensitivities are observed when precipitation is small and the WEET is large. In fact, a ridge of high sensitivities is seen in the plot, which corresponds to the S-shaped curves shown in Figure 4c. This ridge ultimately arises from the opposing impacts of more efficient recharge and smaller portions of the region producing recharge. Notice also that the highest sensitivities of groundwater occur when the groundwater runoff is smallest. Even though the slope of the associated curve in Figure 4c is relatively small, the amount of groundwater produced relative to the precipitation is small enough to control the sensitivity.

[37] Figure 5d shows the sensitivity of the evapotranspiration to precipitation $\Upsilon_{E[\bar{E}],E[\bar{P}]}$. Here again, we observe that the contours are approximately radial from the origin, suggesting that the sensitivity is approximately a function of D_{E_w}. The sensitivity is less than 1 for the entire range of precipitation and WEET shown. In fact, one can use a water balance to show that the sensitivity of evapotranspiration must be less than one if the sensitivities of the surface and groundwater runoff are above one. The highest sensitivities

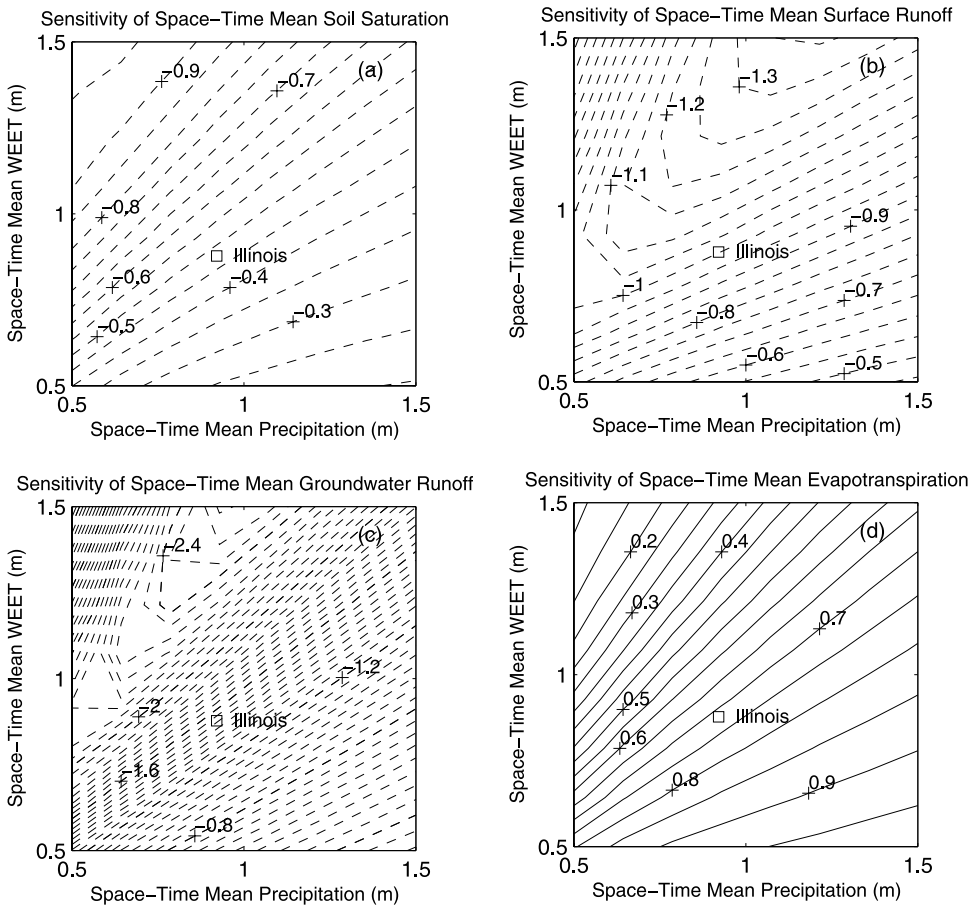

Figure 6. The sensitivities of hydrologic variables to WEET. (a) Sensitivity of soil saturation $\Upsilon_{E[\overline{s}],E[\overline{E}_w]}$, (b) sensitivity of surface runoff $\Upsilon_{E[\overline{R}],E[\overline{E}_w]}$, (c) sensitivity of groundwater runoff $\Upsilon_{E[\overline{G}],E[\overline{E}_w]}$, and (d) sensitivity of evapotranspiration $\Upsilon_{E[\overline{E}],E[\overline{E}_w]}$. All of these plots show contours of their associated sensitivity.

are observed when precipitation is low and WEET is high. The sensitivity for the Illinois basin is about 0.4.

[38] This analysis can be repeated to analyze the sensitivities to WEET (i.e., $\Upsilon_{E[\overline{s}],E[\overline{E}_w]}$, $\Upsilon_{E[\overline{R}],E[\overline{E}_w]}$, $\Upsilon_{E[\overline{G}],E[\overline{E}_w]}$, and $\Upsilon_{E[\overline{E}],E[\overline{E}_w]}$), which are shown in Figure 6. Figures 6a–6d exhibit qualitatively similar contour patterns to those in Figures 5a–5d. However, a few differences are observed. The first difference is that the sensitivities of soil saturation, surface runoff, and groundwater runoff are positive in Figure 5 but negative in Figure 6. The negative sensitivities imply that an increase in WEET results in a decrease in soil moisture, surface runoff, and groundwater runoff, which is expected from intuition. The second major difference is that the surface runoff sensitivity values are typically closer to zero in Figure 6 than in Figure 5. The lower sensitivities indicate that surface runoff production is more dependent on precipitation than WEET. The third major difference is that the highest sensitivity values of evapotranspiration in Figure 6 occur when precipitation is large and WEET is small, whereas this situation produces the lowest sensitivity values in Figure 5. The similarities between the contour patterns in Figures 5 and 6 confirm that the roles of precipitation and WEET are closely related in the model (Section 3 showed that the model depends strongly on the ratio of precipitation to WEET). The similarity between the two types of sensitivities is an important result because it suggests that more detailed studies about the sensitivity to one variable can give qualitative insights into the sensitivity to the other variable. Notice that the sensitivity of evapotranspiration for the Illinois basin is again significantly smaller in magnitude compared to the sensitivities of the runoff components.

[39] So far, we have examined the sensitivities of the regional water balance for the Illinois River basin and hypothetical regions that have differing precipitation and WEET. We now examine how other physical and statistical characteristics of the region impact the sensitivities. Figure 7 plots $\Upsilon_{E[\overline{s}],E[\overline{P}]}$, $\Upsilon_{E[\overline{R}],E[\overline{P}]}$, $\Upsilon_{E[\overline{G}],E[\overline{P}]}$, and $\Upsilon_{E[\overline{E}],E[\overline{P}]}$ as four physical characteristics of the region are varied. Here α/i describes the infiltrability of the soil relative to the mean intensity of precipitation where precipitation occurs. Most of the sensitivities remain relatively constant as α/i varies, but the sensitivity of the surface runoff increases substantially as α/i increases (Figure 7a). As α/i becomes large, Horton runoff becomes weaker and the surface runoff depends more on Dunne runoff (see Figure 2a). Dunne

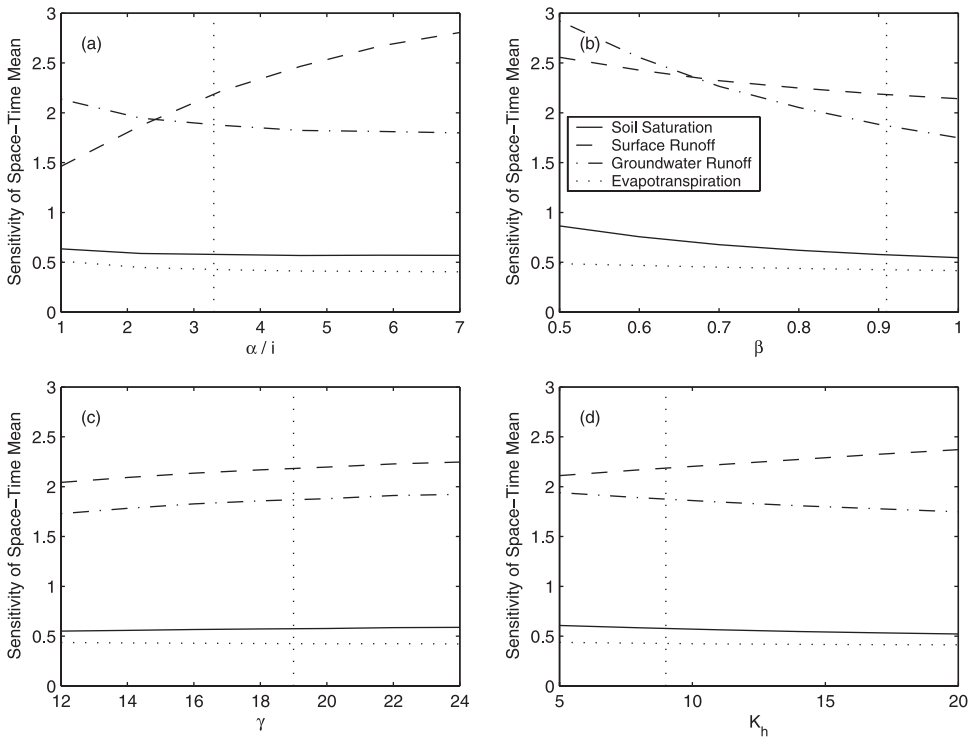

Figure 7. Sensitivities of the space-time mean hydrologic variables to space-time mean precipitation. In Figures 7a–7d the sensitivities are plotted as different values are used for the specified physical characteristic or parameter. The value most representative of the Illinois basin is identified by a vertical dotted line in each plot.

runoff is sensitive to soil saturation, which varies with precipitation. This result suggests that as Dunne runoff becomes more important in a region, the sensitivity of surface runoff to precipitation increases.

[40] The parameter β identifies the soil saturation value that distinguishes moisture-limited and energy/transport-limited evapotranspiration conditions and is largely dependent on the vegetation characteristics. Surprisingly, the value of β has the strongest impact on the sensitivities of surface and groundwater runoff, which are not directly related to β (Figure 7b). As β becomes small, the evapotranspiration efficiency increases (see Figure 2c), which implies that less precipitation becomes surface and groundwater runoff. Therefore the changes in runoff induced by changes in precipitation correspond to higher sensitivities when β is small. In short, evapotranspiration becomes increasingly competitive as β becomes small, which leads to greater sensitivities of surface and groundwater runoff.

[41] Figures 7c and 7d show the four sensitivities as the soil properties γ and K_h are varied. In both cases, the changes in the sensitivities are relatively small, which suggests that these parameters play a relatively weak role in determining the impact of climate changes on the water balance within the range of values tested. It should be noted that K_h can have a much wider range of values between certain regions.

[42] We can also investigate the sensitivities to precipitation as the statistical characteristics of the region change (Figure 8). Figure 8a shows that increasing $\sigma_{\overline{s}}$ causes a substantial decrease in the sensitivity of groundwater runoff. Groundwater runoff has a strong dependence on soil saturation (see Figure 2b). The parameter $\sigma_{\overline{s}}$ has the effect of smoothing the relationship between groundwater runoff and soil saturation, thus reducing the sensitivity to changes in soil saturation or precipitation. Increasing k tends to increase the sensitivity of groundwater runoff (Figure 8b). As k increases, the variability of the soil moisture in space is reduced, so the sensitivity of groundwater runoff increases. Figures 8c and 8d also adhere to this reasoning. As $\sigma_{\overline{P}}$ or $\sigma_{\overline{E}_w}$ increases, the sensitivities decrease because the variability represented in the hydrologic system increases. In these cases, however, the sensitivities change only a small amount because the effects of these parameters are modulated by the correlations between the variables and soil moisture (i.e., $\rho_{\overline{P},\overline{s}}$ and $\rho_{\overline{E}_w,\overline{s}}$; see equations (14) and (16)). The correlations can also affect the sensitivities, but significant changes in the sensitivities would require rather extreme and unlikely correlation values (Figures 8e and 8f).

[43] We have performed the same analyses for the sensitivities to WEET (i.e., $\Upsilon_{E[\overline{s}],E[\overline{E}_w]}$, $\Upsilon_{E[\overline{R}],E[\overline{E}_w]}$, $\Upsilon_{E[\overline{G}],E[\overline{E}_w]}$, and $\Upsilon_{E[\overline{E}],E[\overline{E}_w]}$). The results tend to be approximate mirror images of those in Figures 7 and 8, although the exact shapes of the curves can be rather different. For example, when α/i increases, the sensitivity of the surface runoff to precipitation becomes more positive (larger), but the sensitivity to WEET becomes more negative. Similarly, an increase in $\sigma_{\overline{s}}$ results in a less positive (smaller) sensitivity of groundwater runoff to precipitation and a less negative sensitivity of groundwater runoff to WEET. The temporal

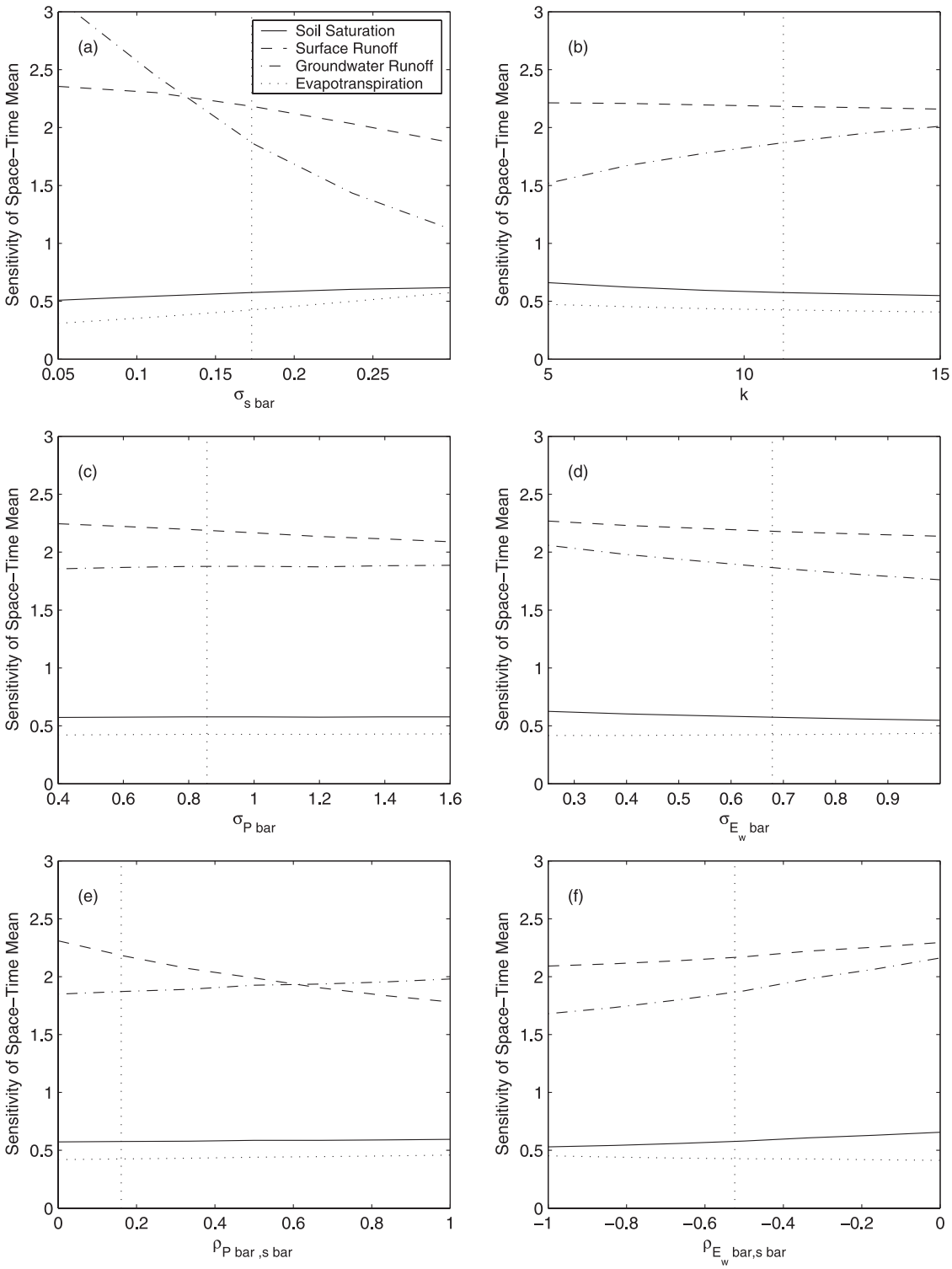

Figure 8. Sensitivities of the space-time mean hydrologic variables to space-time mean precipitation. In Figures 8a–8f the sensitivities are plotted as different values are used for the specified statistical property. The value most representative of the Illinois basin is identified by a vertical dotted line in each plot.

standard deviations and correlations have very little impact on the sensitivities to WEET.

[44] It should be emphasized that the analyses in this section consider the sensitivities when only one of the region's physical or statistical properties changes. In some cases, one might expect values of certain parameters to be related (for example, both γ and K_h vary with soil texture). Simultaneous changes in the model parameters may have

more or less significant impacts on the sensitivities than the individual changes described here.

5. Conclusions

[45] For a range of climatic conditions, the results of this study suggest that runoff processes tend to amplify climate change signals in precipitation and WEET while evapotranspiration processes tend to dampen the same signals. These results are consistent with the fact that runoff depends on precipitation intensity exceeding the capacity of the soil to transport and store water. The dynamics of such an excess-based process are likely to be more sensitive than those of evapotranspiration, which relies on access to water stored in the soil, which is found to be relatively stable under the climate changes tested. Furthermore, regions where Dunne runoff is the dominant mechanism of surface runoff production exhibit higher sensitivities to changes in precipitation and WEET. The increased sensitivity occurs because changes in precipitation induce changes in soil saturation, which affects Dunne runoff production. In contrast, Horton runoff depends mainly on the rainfall intensity during a precipitation event. Horton runoff is therefore expected to be less sensitive to climate changes unless the mean intensity of precipitation during storm events changes along with the region's space-time mean precipitation. For the Illinois basin, a 1% increase in precipitation is expected to cause roughly a 2.2% increase in surface runoff, a 1.9% increase in groundwater runoff, and a 0.4% increase in evapotranspiration. A 1% increase in WEET is expected to cause roughly a 1.0% decrease in surface runoff, a 1.5% decrease in groundwater runoff, and a 0.7% increase in evapotranspiration. These conclusions have important implications in guiding attempts to detect climate changes in the water cycle. For the conditions tested here, runoff is usually more sensitive than soil moisture or evapotranspiration and therefore should reflect climate signals more readily. In fact, the sensitivities of surface and groundwater runoff to precipitation are above one, which suggests that climatic changes in precipitation should be more readily observed by changes in the runoff than in the precipitation itself.

[46] Among the sensitivities studied, the sensitivities of the groundwater runoff vary the most between regions with differing mean precipitation and mean WEET. This result suggests that the response of groundwater to climate change may be difficult to predict and represents an important avenue for further research. Also, physical characteristics that control the behavior of the evapotranspiration process can have a stronger impact on the sensitivity of the groundwater runoff production than the evapotranspiration itself. In particular, the vegetation-dependent parameter β is used to differentiate moisture-limited and energy/transport-limited evapotranspiration conditions, but this parameter has a stronger role in determining the sensitivity of groundwater runoff than evapotranspiration (Figure 7b). This surprising behavior occurs in part because evapotranspiration is a relatively efficient process in accessing water from the soil storage. Other physical and statistical characteristics have little impact on the sensitivities within the range of values tested, including the temporal standard deviations of precipitation and WEET and the correlations between these variables and soil moisture. Simultaneous changes in multiple regional characteristics were not tested and may have more or less significant impacts on the sensitivity results. In addition, these characteristics might impact other hydrologic properties such as the sensitivity of extreme values of runoff.

[47] The probabilistic model used in this analysis depends on two humidity indices: $D_{E_w} \equiv E[\overline{P}]/E[\overline{E}_w]$ and $D_{K_h} \equiv E[\overline{P}]/K_h$. Among these two indices, D_{E_w} has the stronger influence, which is consistent with the fact that empirical expressions for mean evapotranspiration efficiency and mean runoff coefficient are commonly written in terms of D_E (which is similar to D_{E_w}). Because D_{E_w} is the dominant variable in determining the mean fluxes and mean soil saturation, the sensitivities of these variables to mean precipitation are qualitatively related to the sensitivities to mean WEET. For example, regions with the most severe sensitivities of mean soil moisture to mean precipitation also have the most severe sensitivities to mean WEET (although the signs are opposite).

[48] **Acknowledgments.** We gratefully acknowledge financial support from the U.S. Army Research Office and the thoughtful comments of four reviewers.

References

Bain, L. J., and M. Engelhardt (1992), *Introduction to Probability and Mathematical Statistics*, PWS-KENT, Boston, Mass.

Bouchet, R. J. (1963), Evapotranspiration reelle et potentielle, signification climatique, *Int. Assoc. Sci. Hydrol. Publ.*, *62*, 134–142.

Brutsaert, W., and H. Strickler (1979), An advection-aridity approach to estimate actual regional evapotranspiration, *Water Resour. Res.*, *15*(2), 443–450.

Budyko, M. I. (1950), Climatic factors of the external physical-geographical processes (in Russian), *GI Geofiz. Observ.*, *19*, 25–40.

Campbell, G. S. (1974), A simple method for determining unsaturated conductivity from moisture retention data, *Soil Sci.*, *117*(6), 311–314.

Clapp, R. B., and G. M. Hornberger (1978), Empirical equations for some soil hydraulic properties, *Water Resour. Res.*, *14*(4), 601–604.

Cosh, M. H., and W. Brutsaert (1999), Aspects of soil moisture variability in the Washita '92 study region, *J. Geophys. Res.*, *104*(D16), 19,751–19,757.

Dooge, J. C. I. (1992), Sensitivity of runoff to climate change: A Hortonian approach, *Bull. Am. Meteorol. Soc.*, *73*(12), 2013–2024.

Dooge, J. C. I., M. Bruen, and B. Parmentier (1999), A simple model for estimating the sensitivity of runoff to long-term changes in precipitation without a change in vegetation, *Adv. Water Resour.*, *23*, 153–163.

Dunne, T., and R. D. Black (1970), Partial area contributions in a small New England watershed, *Water Resour. Res.*, *6*(5), 1296–1311.

Eltahir, E. A. B., and R. L. Bras (1993), Estimation of fractional coverage of rainfall in climate models, *J. Clim.*, *6*, 639–644.

Entekhabi, D., and P. S. Eagleson (1989), Land surface hydrology parameterization for atmospheric general circulation models, *J. Clim.*, *2*, 816–831.

Entekhabi, D., and P. S. Eagleson (1991), Climate and the equilibrium state of land surface hydrology parameterizations, *Surv. Geophys.*, *12*(1-3), 205–220.

Feddes, R. A., P. J. Kowalik, K. K. Malinka, and H. Zaradny (1976), Simulation of field water uptake by plants using a soil water dependent root extraction function, *J. Hydrol.*, *31*, 13–26.

Freeze, R. A. (1974), Streamflow generation, *Rev. Geophys.*, *12*(4), 627–647.

Freeze, R. A., and J. A. Cherry (1979), *Groundwater*, 604 pp., Prentice-Hall, Upper Saddle River, N. J.

Hewlett, J. D. (1961), Watershed management, *Rep. 61–66*, Southeast. For. Exp. Stn., Asheville, N. C.

Hewlett, J. D., and R. A. Hibbert (1965), Factors affecting the response of small watersheds to precipitation in humid areas, paper presented at International Symposium on Forest Hydrology, Pa. State Univ., University Park.

Hobbins, M. T., J. A. Ramirez, T. C. Brown, and L. H. J. M. Claessens (2001a), The complementary relationship in estimation of regional eva-

potranspiration: Areal evapotranspiration and advection-aridity models, *Water Resour. Res.*, *37*(5), 1367–1387.

Hobbins, M. T., J. A. Ramirez, and T. C. Brown (2001b), The complementary relationship in estimation of regional evapotranspiration: An enhanced advection-aridity model, *Water Resour. Res.*, *37*(5), 1389–1403.

Hobbins, M. T., J. A. Ramirez, and T. C. Brown (2004), Trends in pan evapotranspiration and actual evapotranspiration across the conterminous U.S.: Paradoxical or complementary?, *Geophys. Res. Lett.*, *31*, L13503, doi:10.1029/2004GL019846.

Hollinger, S., and S. Isard (1994), A soil moisture climatology of Illinois, *J. Clim.*, *7*, 822–833.

Holtan, H. N. (1965), A model for computing watershed retention from soil parameters, *J. Soil Water Conserv.*, *20*(3), 91–94.

Hubbert, M. K. (1940), The theory of groundwater motion, *J. Geol.*, *48*, 785–944.

Lowry, W. P. (1959), The falling rate phase of evaporative soil moisture loss: A critical evaluation, *Bull. Am. Meteorol. Soc.*, *40*, 605–608.

Milly, P. C. D. (1993), An analytic solution of the stochastic storage problem applicable to soil water, *Water Resour. Res.*, *29*(11), 3755–3758.

Milly, P. C. D. (1994), Climate, soil water storage, and the average annual water balance, *Water Resour. Res.*, *30*(7), 2143–2156.

Molz, F. J. (1981), Models of water transport in the soil-plant system: A review, *Water Resour. Res.*, *17*(5), 1245–1260.

Niemann, J. D., and E. A. B. Eltahir (2004), Prediction of regional water balance components based on climate, soil, and vegetation parameters, with application to the Illinois River basin, *Water Resour. Res.*, *40*, W03507, doi:10.1029/2003WR002851.

Ol'dekop, E. M. (1911), On evaporation from the surface of river basins: Transactions on Meteorological Observations, Lur-evskogo (in Russian), report, Univ. of Tartu, Tartu, Estonia.

Pike, J. G. (1964), The estimation of annual runoff from meteorological data in a tropical climate, *J. Hydrol.*, *2*, 116–123.

Risbey, J. S., and D. Entekhabi (1996), Observed Sacramento basin streamflow response to precipitation and temperature changes and its relevance to climate impact studies, *J. Hydrol.*, *184*, 209–223.

Rodriguez-Iturbe, I., A. Porporato, L. Ridolfi, V. Isham, and D. R. Cox (1999), Probabilistic modelling of water balance at a point: The role of climate, soil, and vegetation, *Proc. R. Soc. London, Ser. A*, *455*, 3789–3805.

Salvucci, G. D., and D. Entekhabi (1995), Hillslope and climatic controls on hydrologic fluxes, *Water Resour. Res.*, *31*(7), 1725–1739.

Sankarasubramanian, A., and R. M. Vogel (2002), Annual hydroclimatology of the United States, *Water Resour. Res.*, *38*(6), 1083, doi:10.1029/2001WR000619.

Sankarasubramanian, A., R. M. Vogel, and J. F. Limbrunner (2001), Climate elasticity of streamflow in the United States, *Water Resour. Res.*, *37*(6), 1771–1781.

Schaake, J. C. (1990), From climate to flow, in *Climate Change and U.S. Water Resources*, edited by P. E. Waggoner, chap. 8, pp. 177–206, John-Wiley, Hoboken, N. J.

Schreiber, P. (1904), Uber die Beziehungen zwischen dem Niederschlag und der Wassfuhrung der Flusse in Mitteleuropa, *Z. Meteorol.*, *21*(10), 441–452.

Schulz, K., and K. Beven (2003), Data-supported robust parameterisations in land surface-atmosphere flux predictions: Towards a top-down approach, *Hydrol. Processes*, *17*, 2259–2277.

Shuttleworth, W. J. (1993), Evaporation, in *Handbook of Hydrology*, edited by D. R. Maidment, chap, 4, pp. 4.1–4.53, McGraw-Hill, New York.

Tadikamalla, P. R. (1990), Kolmogorov-Smirnov type test-statistics for the gamma, Erlang-2 and the inverse Gaussian distributions when the parameters are unknown, *Commun. Stat. Simul. Comput.*, *19*(1), 305–314.

Turc, L. (1954), Le bilan d'eau des sols: Relation entre la precipitation, l'evaporation et l'ecoulement, *Ann. Agron.*, *5*, 491–569.

Western, A. W., G. Bloschl, and R. B. Grayson (1998), Geostatistical characterization of soil moisture patterns in the Tarrawarra catchment, *J. Hydrol.*, *205*, 20–37.

Wolock, D. M., and G. J. McCabe (1999), Explaining spatial variability in mean annual runoff in the conterminous United States, *Clim. Res.*, *11*, 149–159.

Yeh, P. J. F. (2003), Representation of water table dynamics in a land surface scheme: Observations, models, and analyses, Ph.D. dissertation, Mass. Inst. of Technol., Cambridge.

Zhang, L., W. R. Dawes, and G. R. Walker (2001), Response of mean annual evapotranspiration to vegetation changes at catchment scale, *Water Resour. Res.*, *37*(3), 701–708.

E. A. B. Eltahir, Department of Civil and Environmental Engineering, Massachusetts Institute of Technology, Cambridge, MA 02139, USA.

J. D. Niemann, Department of Civil Engineering, Colorado State University, Campus Delivery 1372, Fort Collins, CO 80523-1372, USA. (jniemann@engr.colostate.edu)